

Photocatalytic Removal of O- Nitro Phenol from Wastewater by Novel an Eco-friendly Magnetic Nanoadsorbent

Shirsath D.S. and Shrivastava V.S.*

Nanochemistry Research Laboratory, G.T.Patil College, Nandurbar-425412, (M.S.), India

Received 28 April 2014;

Revised 5 July 2014;

Accepted 18 Oct. 2014

ABSTRACT: Phenols are toxic organic compounds and which badly affects the flora and fauna of the biosphere because phenols are persistent pollutant found in wastewater from many industries. In present research article the photocatalytic removal of O-Nitro Phenol by synthesized Magnetic Nanoadsorbents (MNA) carried out under photocatalytic reactor. The MNA were synthesized by Co-precipitation method required short period of time. The photocatalytic reactor manually assembled in the laboratory. The U.V irradiation found to be effective. The different parameters have been studied like initial concentration of O-Nitro Phenol, temperature, contact time, adsorbent dose and pH. The effective removal of O-Nitro Phenol by MNA at optimum pH 1.5 to 2.5. The employed MNA was characterized by SEM (Scanning Electron microscopy), XRD (X-ray Diffraction) and FTIR (Fourier Transfer Infrared Spectroscopy). The Present removal study well fitted for Freundlich and Langmuir adsorption isotherm. A kinetics and equilibrium studies were also carried out by using MNA. In this experimental research the desorption study of MNA also shows good results, reusability of MNA were possible.

Key words: O-Nitro phenol, Magnetic nanoadsorbents (MNA), Photocatalytic, Flora-fauna

INTRODUCTION

The origin of phenol in the environment is both industrial and natural. Phenol pollution is associated with Pulp mills, coal mines, refineries, wood preservation plants and various chemical industries as well as their wastewater (Paula *et al.*, 19980). Phenols are persistent pollutant found in wastewater from many industries like petrochemical and petroleum refineries, coal, cooking, polymer product, dye synthesis, wood processing plants, pharmaceuticals, pesticides (Gopalkrishnamoorthy *et al.*, 1987). A natural source of phenol includes forest fire, natural runoff water from urban areas where asphalt is used as the binding material and natural decay of lignocellulosic material. The presence of phenol in water imparts carbolic order to receiving water bodies and cause toxic effects on aquatic flora and fauna (Ghadhiet *et al.*, 1995). An organic pollutant comprises a potential group of chemicals which can be dead fully hazardous to human health. Many of these are resistant removal and degradation. As they persist in the environment, they are capable of long range, transportation, bioaccumulation in human animal tissues and biomagnifications of the food chain. The massive mobilization of compounds in natural resources or the introduction of xenobiotics into the

biosphere leads to unidirectional fluxes, which result in the persistence of a number of chemicals in the biosphere and thus constitute a source of contamination. Phenol and its higher homology are aromatic molecules containing a hydroxyl group attached to the benzene ring structure. Mucous membrane is highly sensitive to the action of phenol muscle weakness and tremors are also observed. Acute exposure of phenol causes central nervous system disorders. It leads to collapse and coma. Muscular convulsion is also noted. A reduction in body temperature is resulted and this is known as hypothermia. Phenol causes a burning effect on the skin. Whitening and erosion of skin may also result due to phenol exposer. Phenol has anesthetic effect and causes gangrene. Renal damage and salivation may be included by continuous exposure to phenol. Exposer to phenol may result in irritation of the eye, conjunctions swelling, corneal whitening and finally blindness. Other effects include frothing nose and mouth followed by headache. Phenol can cause hepatic damage also. Chronic exposure may result in anorexia, dermal ash disposal, gastrointestinal disturbance vomiting, weakness, weightlessness, muscle pain, hepatic tenderness and nervous disorder, it is also

*Corresponding author E-mail: drvinod_shrivastava@yahoo.com

suspected that exposure to phenol may cause paralysis, cancer and genital fiber striation. Phenol and its derivatives are toxic and classified as hazardous material. (Zumriye *et al.*, 1999). Phenol is also a priority pollutant and is included in the list of EPA (1979). Phenols are toxic to human beings and affect several biochemical functions (Nuhoglu *et al.*, 2005). Hence, wastewater containing phenol needs careful treatment before it is discharged into receiving body of water, especially when it is to be used for drinking purposes (Autenrieth *et al.*, 1991). Phenols can be treated by various physical-chemical and biological methods (Kai *et al.*, 2000). Physico-chemical methods for phenol removal are costly and cannot remove phenol completely or convert into some other form which may be less harmful. Adsorption on Chitosan is an alternative technology which is versatile, inexpensive and can be potentially turn a toxic material solution into harmless products (Gibson *et al.*, 1968). Phenolic compounds are among the most refractories. Pollutants present in industrial wastewater. Their high stability and solubility in water represent the main obstacles to complete removal. Purification of wastewater contaminated with these pollutants are very difficult since they are resistant to conventional treatment. The largest use of phenol is an intermediate in the production of Phenolic resin. Phenol is also used in the production of caprolactum, which is used in nylon as well as Bisphenol A, which is used in making epoxy and other resin (Luttrell *et al.*, 2003). Moreover, phenol is also used as fungicide, disinfectants, and in medicinal preparation such as over the counter treatment for sore throats. The O-Nitro phenols exert various biochemical and morphological effects on plants and animals. However, there are several techniques like coagulation, Flootation, ion exchange, adsorption, reverse osmosis and biological oxidation, which is used for removal of o-Nitro phenol. One very specific and promising technology for removal of O-Nitro phenol is adsorption on organic-polymer material which has attracted a great deal of attention over the last two decades to restore our ecosystem (Laurent *et al.*, 2008). Therefore, in this investigation MNA has taken as effective adsorbent for the removal of O-Nitro phenol.

The overall benefits of decolorisation and removal of O-Nitro phenol from aqueous media may include interesting subject, saving a huge amount of water, because textile industries are regarded as chemical and water intensive that is these industries are more polluting and consume large amounts of water. The treated water may be recycled and reused in the same industry and agricultural field. The present works report an investigation of adsorption of O-Nitro phenol using MNA. The photocatalytic removal of O-Nitro phenol is a cost effective method of treating industrial

wastewater by using magnetic nonadsorbent to introduce in this study which should be easily prepared in the laboratory.

MATERIALS & METHODS

The Reagents and chemical used in this investigation supplied from LOBA CHEMIE PVT.LTD and O-Nitro phenol supplied by BDH, India Ltd. The O-Nitro phenol has chemical formula $C_6H_5NO_3$. The maximum wavelength of O-Nitro phenol is $\lambda_{max} = 412nm$. and it is an acidic nature. The structure of O-Nitro Phenol is shown bellow. An accurate weighed quantity of O-Nitro phenol was dissolved in double distilled water to prepare stock solutions for different experimental conditions.

The chemical precipitation technique has been used to synthesize magnetic nanoparticles with homogeneous composition and narrow size distribution (Alkhateeb *et al.*, 2005). The stoichiometry amount of salts of $FeCl_3 \cdot 6H_2O$ (AR/ACS) and $FeSO_4 \cdot 7H_2O$ (AR/ACS) obtained from LOBA CHEMIE PVT. LTD. Mumbai-400005, INDIA were dissolved in double distilled water to prepare desired normal solutions, these solutions were mixed in 250 ml round bottom flask (R.B.F) with mechanical stirring on magnetic stirrer (REMMI Motors Ltd. Mumbai). The R.B.f placed in the water bath (LAB HOSP corporation Ltd.) and maintained the reaction temperature up to 322.5K with constant stirring for 25 minutes to get a clear solution of mixed precursor. Add ammonium hydroxide (25% Liq. Ammonia) in above clear solution drop wise, because every drop of Liq. Ammonia makes the solution becomes colloidal, the magnetic particles are seen in the colloidal solution. The synthesis of MNA in this reaction follows the Co-precipitation methods. The magnetic properties of synthesized magnetic particles were examined by taking the simple magnet nearby the R.B.F containing colloidal solution of magnetic particle, it is seen that the colloidal particles attracted towards the magnet strongly, also which confirms the synthesized materials contain the magnetic properties. The stock solution of O-Nitro phenol was suitably diluted to the required initial concentration of O-Nitro phenol with D.D water in each experimental condition. (Morrison *et al.*, 1967). An accurately amount of MNA was added to 50 ml different ppm concentration of O-Nitro phenol solution in 100ml of the beaker and the mixture was agitated in a mechanical shaker on magnetic stirrer at fix rpm for giving time at constant temperature at 27 °c under U.V light for the photocatalytic treatment. The mixture of adsorbent and adsorbate solution centrifuged at 120 rpm. to separate colloidal adsorbent from solution by centrifugation. The absorbance of superman solution was estimated to determine the residual O-Nitro phenol

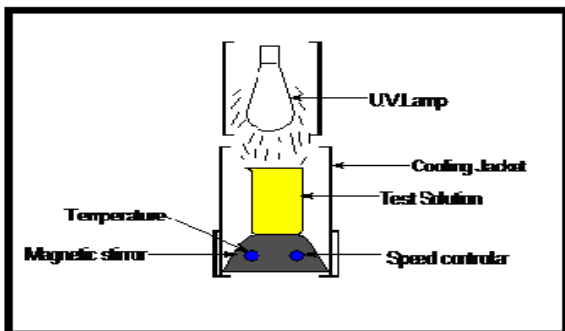


Fig. 1. Showing photocatalytic Reactor removal of O-nitro phenol by using magnetic nanopadsorbent

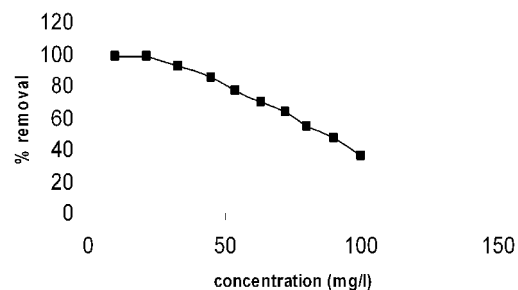


Fig. 2. Effect of initial concentration of O-nitro phenol

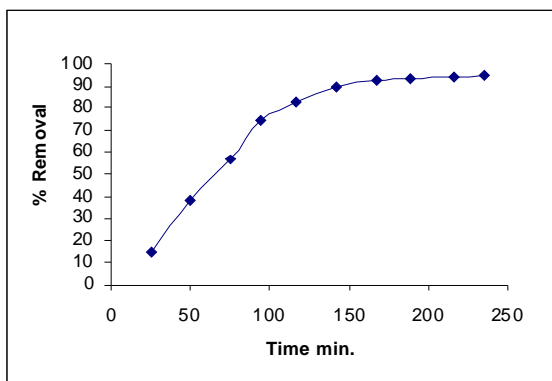


Fig. 3. Effect of contact time on the removal O-nitro phenol

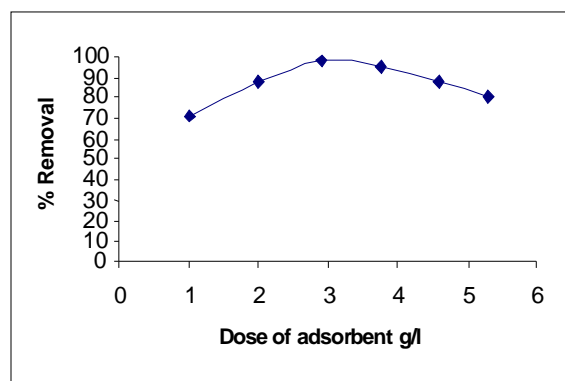


Fig. 4. Effect of dose of adsorbent on the removal of O-nitro phenol

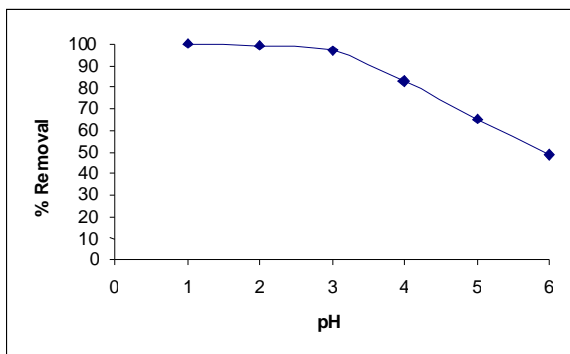


Fig. 5. Effect of different pH on the removal of O-nitro phenol

concentration. The residual O-Nitro phenol concentration was determined using optical density values of before and after photocatalytic treatment at 412 nm with Double beam Spectrophotometer (Systonics -2003) using a quartz cell of 1cm path length. The experiments were carried out at initial pH values ranging from 1 to 10. The pH of the solutions controlled by the addition of 0.1N HCl and 0.1N NaOH solutions. Kinetic photocatalytic of adsorption of O-Nitro phenol

on MNA was determined by analyzing adaptive uptake of O-Nitro phenol from aqueous solution at different intervals of time.

The 50 ml solution of the required concentration 10-100 ppm of O-Nitro phenol was prepared from stock solution and transfer into 100 ml borosyl beaker for U.V irradiation in photocatalytic reactor. Before U.V irradiation 0.2GM of adsorbent was added and stirred in the dark for 15 minutes, so that adsorption equilibrium could be established. The solution was then exposed to the U.V for irradiation with constant stirring throughout the experiment. The photocatalytic reactor constructed by using U.V. Lamp of the desired wavelength with suitable place for the Magnetic stirrer having temperature and speed controller as shown in fig. 1. The lamp fitted to outer cooling jacket and aluminum foil cover which withstand the dye solution from drying. The decolorization efficiency of O-Nitro phenol by MNP was calculated by a mathematical equation adapted from the measurement of decolorization (Hussein *et al.*, 2008). From the respective absorbance obtained, percentage colour disappearance was calculated by using double beam spectrophotometer model no. systonics-2203.

The adsorption of O-Nitro phenol onto MNA was monitored for 250 min. The initial concentration of O-Nitro phenol was 50ppm and 70ppm respectively, the other parameter is kept constant. As seen in fig. 2. O-Nitro phenol was adsorbed onto MNA rapidly and equilibrium was achieved within 145 min., independent of initial of O-Nitro phenol. This could be due to the microspores structure of MNA, which was favorable for the diffusion of the O-Nitro phenol from the bulk solution onto active sites on the MNA surface. The remains of MNA after treatment was used for the dissipation study. Apparently external adsorption dominated and no pore diffusion was observed to slow down the adsorption rate. Fig. 2. % R Vs Concentration. The effect of contact time on the removal of o-Nitro phenol from aqueous solution is presented in fig. 3. The experiments were carried out at 400 rpm 2.0g/l of adsorbent dose at room temperature, normal pH and initial concentration of O-Nitro phenol ranges from 10 to 50ppm (mg/l) for different time interval up to 120 minutes. The percentage removal of O-Nitro phenol increased from 15.58 to 99.86 mg/l for MNA as the concentration of O-Nitro phenol increased from 10 to 50 ppm. The equilibrium was established within 145 minutes for all studied concentration. It is observed that the removal of O-Nitro phenol depends upon its initial concentration. In order to examine the effect of adsorbent dose on the removal efficiency of O-Nitro phenol adsorption, the experiment was set up with varying amount of adsorbent dose 2mg/l, 5mg/l and 10mg/l for MNA, while keeping the concentration of O-Nitro phenol constant and temperature at 300°k and normal pH were constant at different contact time up to 120 minutes. The percentage adsorption increases from 86 to 92.87 as the dose of adsorbent was increased from 1.0g/l to 6g/l. Maximum O-Nitro phenol was sequestered from the solution within 145 minutes after the start of the experiment. A large mass of adsorbent could adsorb large amount of O-Nitro phenol to the availability of more adsorption site and more surface area of adsorbent. Fig. 4 % R Vs adsorbent dose. It is well known that pH is one of the most important factors which affect the adsorption process. An experiment was performed to find the optimum pH on the adsorption of O-Nitro phenol onto MNA using different pH values changing from 1-6. During Present investigation the effect of pH on the adsorption of O-Nitro phenol as seen, the removal of O-Nitro phenol is clearly pH dependent with the highest adsorption occurring at low pH. It is observed that as the pH increases the adsorption capacity of the O-Nitro phenol onto MNA decreases as shown in fig. 5. % R Vs pH.

RESULTS & DISCUSSION

Scanning electron microscopy is widely used to study the morphological features and surface

characteristics of absorbent materials. In this study the adsorbent material was analyzed before and after treatment it shows greater extent of adsorption of O-Nitro phenol. As shown in Fig. 6 a) and Fig. 6 b) and Fig. 7 a) and Fig. 7 b) respectively. The fig. 7 c) shows that most of nanoparticle shows hexagonal structure and some structure shows irregular polygons. The SEM analysis clearly indicates that there is distinct adsorption of O-Nitro phenol is observed after treatment.

The X-ray diffraction analysis shows the major diffraction peaks assigned to related reflection lines and were in good agreement with the literature values for magnetite. The position and intensity count of the diffraction peaks of the sample match well with the standard XRD data for bulk magnetite (JCPDS No. 88-0866). The characteristic peaks appeared at the small peak at 30.1° (220), 35.3° (311), 42.7° (400), 54.7.0° (511) and 62.4° (440) are can be assigned to the peaks of the Fe₃O₄ as shown in fig. 8. (Zhai *et al.*, 2009, Tural *et al.*, 2009). The size of synthesized magnetic nonadsorbent was calculated by Using Scherrer's formula, the crystallite size of the synthesized magnetic nonadsorbent was determined by Scherrer formula Eq. 1. and it is about 45 nm. Other peaks any other some very trace amount of impurities are seen in this pattern, indicating that the high purity of the synthesized magnetic nonadsorbent. Also photograph showing (fig. 9) clearly indicates the synthesized magnetic nonadsorbent contain sufficient magnetic properties. The fig. 10. Shows the absorption spectra of magnetic nonadsorbent.

$$D = K\lambda/\beta\cos\theta \quad (1)$$

The FTIR measurements were performed by using (Lamnda Scientific FTIR-7600) with KBr background over a range of 4000-400 cm⁻¹ to determine magnetic material. The I.R spectra obtained by FTIR with can be help in identifying the chemical composition or bonding present in the newly synthesized molecule. The FTIR provides the tool that contains structural information about the presence of certain functional groups in the unknown molecule. The frequency at 587.0cm⁻¹ as shown in FTIR graph Fig. 11. It clearly indicates that the unknown molecule is Fe₂O₃ group.

The peak at 3390.77cm⁻¹ is due to the presence of moisture in KBr and some small noised peaks are due to the presence of impurities in magnetic nanoparticles. In order to investigate the mechanism of sorption several kinetics models were tested, including pseudo first order model and pseudo-second order model. The Lagergrens rate equation is most widely used (Battacharya *et al.*, 2003) for the adsorption of adsorbate from solution.

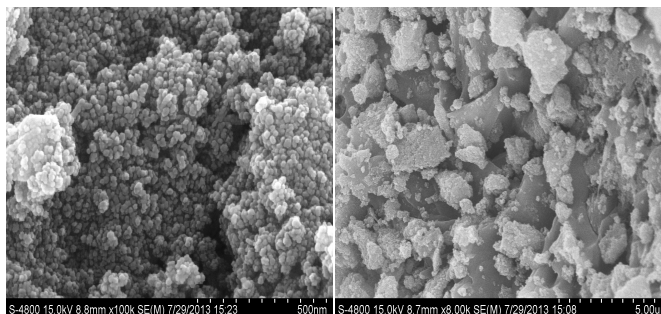


Fig. 6.a) Before Treatment

Fig. 6. b) After Treatment

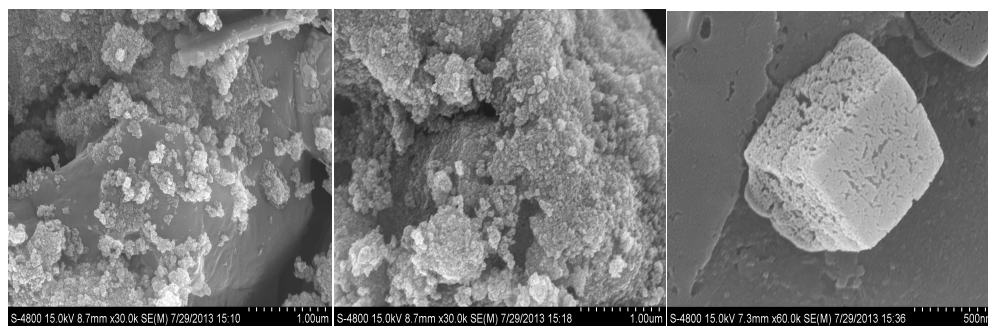


Fig. 7 a) Before Treatment

Fig. 7. b) After Treatment

Fig. 7 c) SEM image of magnetic nanoadsorbent (MNA)

The first order Lagergrens rate equation is as follows

$$\ln(q_e - q_t) = \ln q_e - k_1 t \quad (2)$$

Where q_e (mg/g) and q_t (mg/g) are the amount of O-Nitro phenol adsorbed at equilibrium and at time t , respectively, and k_1 is the first order rate constant (min^{-1}). The values of k_1 were calculated from plots of $\ln(q_e - q_t)$ Vs. t as shown in fig. 12. for different concentration of O-Nitro phenol.

Pseudo second order equation (Ho *et al.*, 1999) based on equilibrium adsorption is expressed as:

$$t/q_t = 1/k_2 q_e^2 + t/q_e \quad (3)$$

Where k_2 (g/mg min) is the rate constant of second order adsorption. If second order is applicable, the plot of t/q_t Vs t should show a linear relationship. q_e and k_2 can be determined from the slope and intercept of the plot respectively. The linear plot of t/q_t Vs t is represented in fig. 13 show a good agreement between experimental q_e and calculated q_e values. The correlation coefficient for the second order kinetics model are greater than 0.98 and experimental q_e values agree with the calculated ones indicating the applicability of this kinetics equation, this can be determined from the table no.1. This shows that the adsorption process of O-Nitro phenol onto MNA is a second order nature. The relationship between initial O-Nitro phenol

concentration and adsorption percentage of O-Nitro phenol are shown in fig. 2. When the concentration was increased from 50 to 70 ppm. The percentage of adsorption O-Nitro phenol 96.34% to 80.45% and 97.54% to 65.35%, respectively, with the data in fig. 14. The Langmuir equation was employed to study the adsorption isotherm of O-Nitro phenol. The Langmuir equation is based on the assumption that maximum adsorption corresponds to saturate monolayer of the adsorbate molecule on the adsorbent surface, that the energy of adsorption is constant.

The Langmuir equation was shown as follows.

$$C_e/q_e = 1/(a.Q_m) + C_e/Q_m \quad (4)$$

Where C_e ppm is the concentration of O-Nitro phenol containing solution at equilibrium we be the amount O-nitrophenol adsorbed at equilibrium in ppm. Q_m is the maximum adsorption and a is the Langmuir constant. Where q_m and a value is obtained from the slope ($1/Q_m$) and intercept ($1/a.Q_m$) of the linear plot of C_e/q_e Vs C_e . The straight lines Langmuir equation, the values of parameter and the correlation coefficient of Langmuir equation of O-Nitro phenol adsorbed on MNA are given in table no.2 The experimental evidences are shown that the adsorption isotherm of O-Nitro phenol adsorbed on MNA is fit for Langmuir model. The (Q_m) maximum adsorption capacity of the MNA for O-Nitro phenol was 298.32 mg/g. Whole data

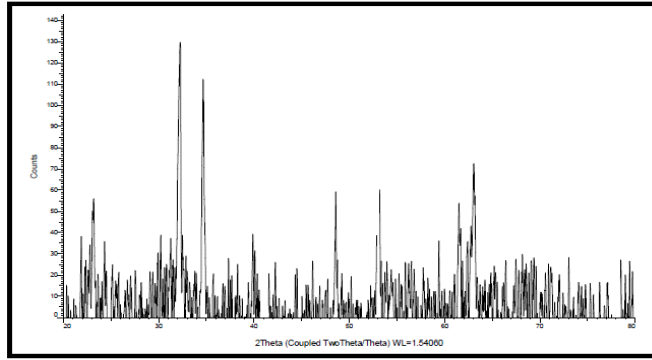


Fig. 8. XRD Pattern of Magnetic Nanoadsorbent (MNA)

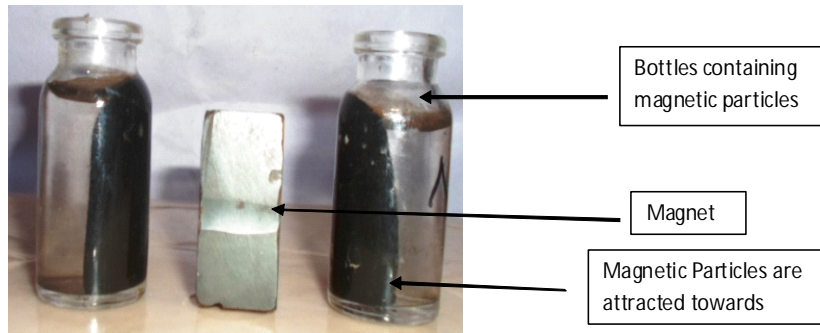


Fig. 9. Photograph showing tentative determination of magnetic properties in synthesized magnetic nanoadsorbent (MNA)

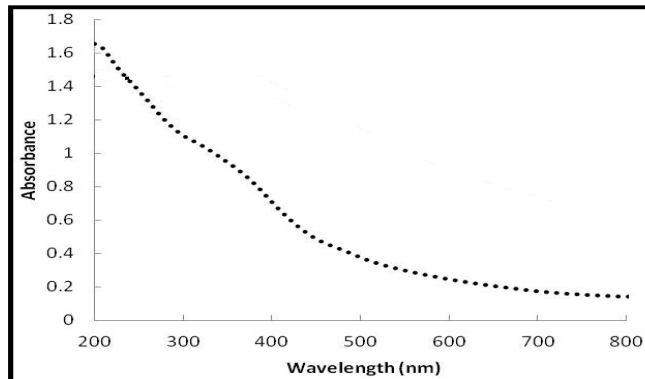


Fig. 10. The absorption spectra Fe_3O_4 magnetic nanoadsorbent.

of maximum adsorption and Langmuir model is shown in fig. 14. One of the most important characteristics of an adsorbent is the amount of adsorbent it can accumulate, which is calculated from the adsorption isotherms. Adsorption isotherms are constant-temperature equilibrium relationship between the amount of adsorbent per unit of adsorbent (Q_e) and its equilibrium solution concentration (C_e) as shown in fig. 15. A number of mathematical models have been employed for describing this equilibrium relationship. Out of several models, Freundlich and Langmuir models have been reported most frequently.

(Langmuir *et al.*, 1916, Freundlich *et al.*, 1906). Eqs. (5) and (6) represent the Freundlich and the Langmuir models, respectively. The linear forms of the Freundlich and the Langmuir models are given by Eq. (7)

$$Q_e = K_F C_e^{1/n} \quad (5)$$

$$Q_e = Q_m K_L C_e / (1 + K_L C_e) \quad (6)$$

$$\log Q_e = \log K_F + 1/n \log C_e \quad (7)$$

Where Q_e is the amount of O-Nitro phenol adsorbed onto the MNA (mmol/g), C_e is the equilibrium concentration of O-Nitro phenol in the supernatant

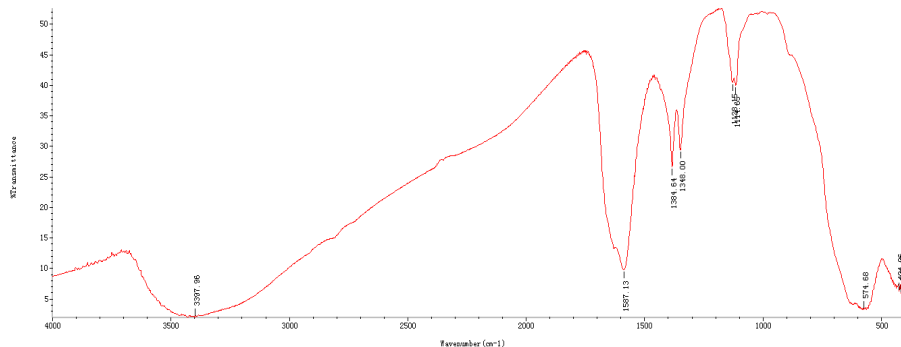


Fig. 11. FTIR pattern of Magnetic nanoadsorbent (MNA)

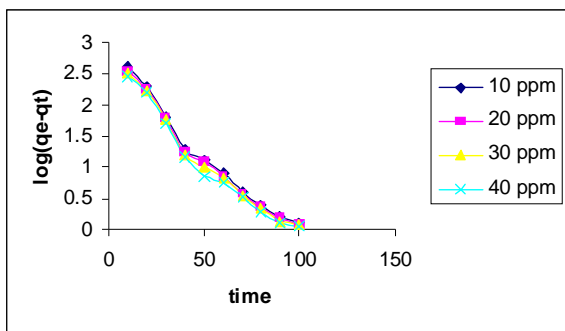


Fig. 12. Pseudo First Order kinetics of O-nitro phenol Adsorption on Magnetic nanoadsorbent.

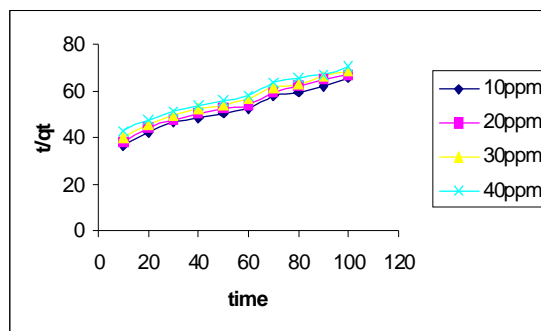


Fig. 13. Pseudo second order kinetics for Adsorption of O- nitro phenol on MNA.

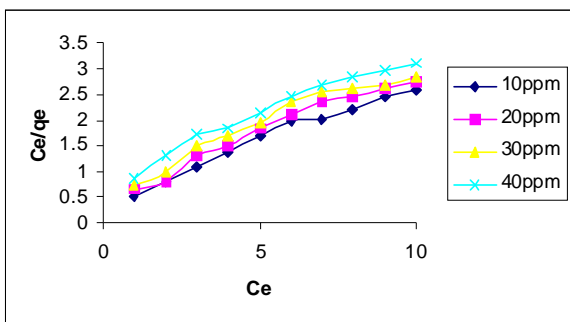


Fig. 14. Langmuir isotherm for adsorption of O-nitro phenol on MNA.

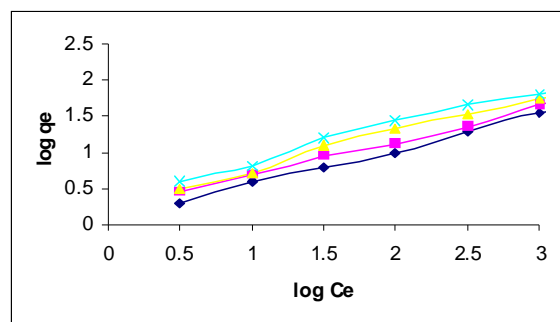


Fig. 15. Freundlich isotherm for adsorption of O-nitro phenol on MNA

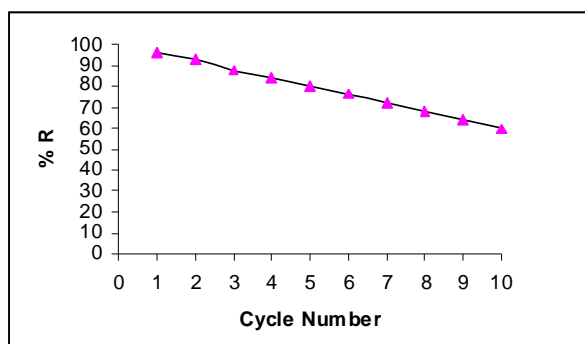


Fig. 16. Reusability of MNP for adsorption/desorption of O-nitro phenol during ten cycles.

Table 1. Comparison of the pseudo first order and pseudo second order adsorption rate Constant and calculated and experiments q_e values for different initial concentration.

O-nitrophenol Concentration/ppm	Adsorbent	q_e (exp)	First order kinetics		
			K_1	q_e (Cal)	r^2
20		3.87	0.079	3.85	0.961
50		3.83	0.058	3.79	0.958
80		2.91	0.053	3.71	0.955
O-Nitro phenol Concentration/ppm		q_e (exp)	K_2	q_e (Cal)	r^2
20		3.89	0.032	3.91	1
50		3.81	0.022	3.82	0.995
80	MNA	3.79	0.021	3.78	0.998

Table 2. Langmuir and Freundlich isotherm models constant and correlation coefficient for adsorption of O-Nitro phenol on prepared MNA.

Adsorbent	Langmuir isotherm			Freundlich isotherm		
	Q_0 (mg/g)	B (l/g)	r^2	K_f	$1/n$	r^2
	3.3	0.497	0.965	5.207	0.25	0.980
	2.99	0.504	0.969	3.785	0.375	0.985
MNA	2.93	0.512	0.973	2.15	0.491	0.99

(mM), K_F and n are Freundlich constants. K_F is roughly an indicator of the adsorption capacity ((mmol/g) (L/mmol) $^{1/n}$), and $1/n$ is the adsorption intensity factor (unitless). Specifically, a larger K_F value suggests a greater adsorption capacity, which is shown in table no. 2, and a lower $1/n$ value indicates stronger adsorption strength. The adsorption isotherms were determined using batch tests at different temperature.

pH measurement were performed with a aliquot of 0.1M HCl and 0.1 M NaOH were used to adjust the over the range of 1-10 pH. In adjusting pH, care was taken not to change significantly the initial concentration of O-Nitro phenol in solution. Therefore, different NaOH and HCl solution of optimum concentration were used to achieve the desired pH values mentioned above.

In this experiment, desorption of O- Nitro phenol form MNA was performed using NaOH solution at different ppm concentration. MNA adsorbed with O-Nitro phenol was exposed to 10ml solution of different NaOH concentration. The mixture was agitated at 200 rpm and 298K in thermostat oven for two hrs. After desorption the MNA adsorbent was separated by simple filtration method. The % of desorption was calculated by following equation

$$\% R = (C_{des}/C_{ads}) \times 100 \quad (8)$$

Where C_{des} and C_{ads} are the amount of O-Nitro Phenol Desorbed from MNA into the aqueous solution and amount of O-Nitro Phenol adsorbed from the aqueous solution onto to MNA respectively.

The removal efficiency, $R(\%)$, O-Nitro phenol, during a ten cycles of adsorption desorption-regeneration, from a 10-mL solution of initial O-Nitro phenol concentration at pH between 6.5 As seen in fig. 16. No significant decrease in the adsorption capacity of the MNA adsorbent during the ten cycles was observed. The results demonstrated that MNA adsorbent can be used for the removal and recovery of O-Nitro phenol from aqueous solution over a number of cycles, indicating its suitability for the design of a continuous process. It is noted that commercially available adsorbents such as, activated carbons are costly, time-consuming and its regeneration is essential. Actually, the regeneration and recovery of spent activated carbons are the most expensive part of the adsorption technology and it accounts for about 75% of the total operating and maintenance costs (Inglezakis *et al.*, 2006). However, it seems this is not the case for the regeneration of spending MNA adsorbent. Therefore, MNA adsorbent is a cost-effective and alternative with fast adsorption rate and its regeneration is simple and may be not necessary, especially for in situ application.

CONCLUSIONS

In the present investigation the MNA were prepared from the Salt of Fe^{+2} and Fe^{+3} have been used as a precursor MNP synthesis employed for the photo catalytic removal of O-Nitro phenol from the aqueous solutions. Adsorption was influenced by various parameters such as Initial pH Initial O-Nitro phenol concentration, contact time and adsorbent dose. The maximum adsorption of O-Nitro phenol by MNA occurred at pH 1.5 to 2.5. for the O-Nitro phenol. Removal efficiency, increased with decreasing the O-Nitro phenol concentration and increasing doses of adsorbent. The Langmuir and Freundlich adsorption isotherm models were used for the description of the adsorption equilibrium of O-Nitro phenol onto MNA. The data were good agreement with Langmuir and Freundlich isotherms. It was shown that the adsorption of O-Nitro phenol on to MNA best fitted by pseudo first order and pseudo second order kinetics.

The adsorbent was characterized by SEM and FTIR to detect adsorption capacity by SEM and by the IR detect frequencies of different functional groups of MNA. This adsorption process is very important to liable for the textile and organic synthesis industrial wastewater treatment.

ACKNOWLEDGEMENTS

Authors are gratefully acknowledged to Shri. G. H. Raisoni Doctoral Fellowship at North Maharashtra University, Jalgaon for Financial Support and North Maharashtra University, Jalgaon for SEM studies. Thanks are also due to Dr. Z. Benzo, IVIC, Caracas, and Venezuela for useful discussions. Authors are also thankful to the Principal G.T.P. College, Nandurbar for providing necessary laboratory facilities and FTIR characterization.

REFERENCES

Alkhateeb, A. N., Hussein, F. H. and Asker, K. A. (2005) Photocatalytic decolonization of industrial wastewater under natural weathering conditions. *Asian J. Chem.*, **72** (2), 1155-1159.

Autenrieth, J. S. and Borner, A. (1991) Biodegradation of Phenolic wastes. *J. Hazardous Materials.*, **28**, 29-53.

Battacharya, K. G. and Sarma, A. (2003) Adsorption characteristic of the dye, Brilliant Green, on Neem leaf powder. *dyes and Pigments.*, **57**, 211-222.

Freundlich, H. M. F. (1906) Uber die adsorption in losungen. *Z. Phys. Chem.*, **57**, 385-470.

Gibson, D. T. (1968). Microbial degradation of aromatic compounds. *Science.*, **161**, 1093-1097.

Ghadhi, S. C. and Sangodkar, U. M. X. (1995). Potential of pseudomonas capacia PPA in bioremediation of aquatic waste containing phenol. proceeding of National symposium frontiers in applied and environmental microbiology. Dec. Cochin., 11-13.

Gopalkrishnamoorthy, H. S. and Shanmugam, T. (1987) Study of the removal of phenol from effluent of low temperature carbonization of lignite plant by resins. *J. Environ. Prot.*, **7** (5), 352-354.

Ho, Y. S. and McKay, G. (1999). Pseudo-second order model for sorption Process. *Process Biochem.*, **34**, 450-465.

Hussein, H. F., Alkhateeb, N. A. and Ismail, K. J. (2008) Solar photolysis and photocatalytic decolorization of thymol Blue. *E-journal of chemistry*, **5**, 243-250.

Inglezakis, V. J. and Pouloupoulos, S. G. (2006) Adsorption, Ion Exchange and Catalysis: Design of Operations and Environmental Applications Elsevier., UK.

Kai, C. L., Chong, T. S. and Wei, F. A. (2000) Immobilized cell membrane Bioreactor high strength Phenol wastewater. *J. Environ. Eng.*, **126**, 75-79.

Langmuir, I. (1916). The constitution and fundamental properties of solids and liquids. Part I. Solids. *J. Am. Chem. Soc.*, **38**, 2221-2295.

Laurent, S., Forge, D., Port, M., Roch, A., Robic, C., Vander Elst, L. and Muller, R. N., (2008). Magnetic iron oxide nanoparticles: synthesis, stabilization, vectorization, physicochemical characterizations, and biological applications. *Chem. Rev.*, **108**, 2064-2110.

Luttrell, W. E. (2003). Toxic Tips: Phenol. *J. Chemical health and safety.*, **10**, 20-21.

Morrison, S. R. and Freund, T. J. (1967). Chemical role of holes and ZnO photocatalysis. *J. Chem. Phys.*, **47**, 1543-1551.

Nuhoglu, A. and Yakin, B. (2005), Modeling of phenol removal in a bath reactor. *Proc. Biochem.*, **40**, 233-239.

Paula, M. V. and Schci Young, L. Y. (1998) Isolation and characterization of phenol degrading denitrifying bacteria. *Appl. Environ. Microbiol. Appl. Environ. Microbiol.*, **64** (7), 23-38.

Tural, B. Ozkan, N. And Volkan, M. J. (2009). Preparation and characterization of polymer coated superparamagnetic magnetite nanoparticle agglomerates. *J. Phys. Chem. Solids.*, **70** (5), 860-866.

Zhai, Y. Liu, F., Zhang, Q. and Gao. G. (2009). Synthesis of magnetite nanoparticle aqueous dispersions in an ionic liquid containing acrylic acid anion. *Col. Surf. A: Physicochem. Eng. Aspects.*, **332**, 98–102.

Zumriye, A. and Gultac, B. (1999). Determination of effective diffusion coefficient of Phenol in calcium alginate immobilized *Pseudomonas putida*. *Enzyme microbial. Technol.*, **25**, 344-348.